



# Enhancing sustainable composites: isolation of nanocellulose from *Selenicereus undatus* (dragon fruit) and kenaf fiber reinforcement in vinyl ester matrix—a study on mechanical, wear, fatigue, creep, and dynamic mechanical properties

R. Ashok Raj<sup>1</sup> · K. Vinoth Kumar<sup>2</sup> · Rajkumar Subburathinam<sup>3</sup> · H. Vinoth Kumar<sup>4</sup>

Received: 25 February 2024 / Revised: 17 April 2024 / Accepted: 27 April 2024 / Published online: 8 May 2024  
© The Author(s), under exclusive licence to Springer-Verlag GmbH Germany, part of Springer Nature 2024

## Abstract

This study explores the potential of utilizing nanocellulose extracted from *Selenicereus undatus* (dragon fruit) and kenaf fiber to enhance the properties of vinyl ester composites. With a focus on sustainable and high-performance materials, our research aims to innovate by reinforcing composites with bioderived nanocellulose and natural fibers. We employ traditional hand layup techniques for precise assembly and abrasive water jet machining for accurate specimen preparation, merging conventional fabrication methods with advanced material science. The integration of nanocellulose and kenaf fibers is expected to significantly enhance the mechanical durability and environmental resistance of the composites, addressing both performance and sustainability concerns. Our comprehensive analysis, following ASTM standards, evaluates mechanical, wear, fatigue, creep, and dynamic mechanical properties of the developed composites. The standout composite, designated VC2, exhibits notable performance improvements, including a tensile strength of 162 MPa, flexural strength of 191 MPa, and impact energy absorption of 5.12 J, among others. Furthermore, VC3 demonstrates exceptional fatigue resistance, while VC4 shows reduced creep strain, highlighting the material's resilience under cyclic loading and prolonged stress. These findings underscore the synergistic effects of combining nanocellulose and kenaf fibers within a vinyl ester matrix, resulting in marked enhancements in both mechanical properties and durability. The successful application of these biobased reinforcements opens new avenues for sustainable composite materials across industries, from automotive to aerospace. This research not only advances our understanding of biocomposite materials but also demonstrates the feasibility of incorporating agricultural waste products into high-value engineering applications. Future studies will focus on optimizing composite formulation and exploring scalability for commercial use, further advancing the field of sustainable material science.

**Keywords** Polymers · Composites · Biomass · Natural fibers · Mechanical properties · Fatigue behavior

## 1 Introduction

The biomass extracted fiber or filler particulates are gaining interest presently, due to their possibility of producing non-toxicity, biodegradability, renewability, and sustainability materials [1]. Generally, this biomass is a non-edible residue from agricultural industry; earlier it was being considered environment pollution-creating substance. But now it has been utilized for obtaining various biofuel and biofiller particulates such as cellulose, biocarbon, biosilica, and lignin [2, 3]. Among these compositions, the cellulose is considered a better source of replacement for petrochemical products in composite field, and it is classified as having fibrillated nanocellulose and crystalline nanocellulose.

✉ R. Ashok Raj  
ashoknoveltyguy@gmail.com

<sup>1</sup> Department of Mechanical Engineering, J.J. College of Engineering and Technology, Trichy, Tamil Nadu, India

<sup>2</sup> Mechanical Engineering, R.M.K. College of Engineering and Technology, Chennai, Tamil Nadu, India

<sup>3</sup> Department of Aeronautical Engineering, Dhanalakshmi Srinivasan Engineering College (Autonomous), Perambalur, Tamil Nadu, India

<sup>4</sup> Department of Mechanical Engineering, M. Kumarasamy College of Engineering, Karur, Tamil Nadu, India

Moreover, the crystalline nanocellulose has enhanced properties when compared to the fibrillated cellulose. This is because of their well-packed long cellulose chain structure along with side-by-side strong hydrogen bonds present on it [4]. The presence of strong hydrogen bonds within the cellulose promotes even dispersion of particle, as well as even loads distribution. Mostly, these features of cellulose particle are naturally present in the plant cell. One such plant species is *Selenicereus undatus* growing in most part of the tropical and sub-tropical region, and it belongs to the cactus family. Here the fruit from this species commonly called as dragon fruit contained cellulose and lignin-like composition within it [5].

Especially, the waste outer cover contained a small leaf-like part which represents yellow, green pigmentation and which represents the presence of cell wall containing cellulose substances. This inherent presence of cellulose in agricultural plant biomass has made an opportunity to research scientists to study about crystalline nanocellulose and which could be utilized for various applications in composite material [6]. Bosenbecker et al. [7] have conducted a study on mechanical characterization of HDPE reinforced with cellulose from rice husk biomass. The rice husk cellulose addition of 10 wt.% has profoundly improved impact strength as well as elastic modulus of the composite. Similarly, microcrystalline cellulosic filler from *Borassus flabellifer* flower of size 70.73 nm reinforced polymer composite was evaluated by Sunesh et al. [8]. The authors found out that the addition of this fine sized microcrystalline cellulose has significantly increased the mechanical, thermal stability properties of the composite material. Furthermore, Nagarajan et al. [9] have investigated the effects of agrowaste cellulosic micro filler reinforced composite material and their mechanical and thermal properties. The study concluded that addition of 15 wt.% of cellulosic filler into composite shows enhanced mechanical and thermal properties. Based on the above literature studies, it is known that the addition of crystalline cellulose into the composite could potentially enhance properties of the material.

Moreover, there is a raise in concern towards achieving sustainable development goals among the nation; the natural fibers are researched and being utilized actively in most of industrial application. In addition to the environmental protection, the natural fiber utilization also improved the strength and stability of the material, and this makes people to switch towards the natural fiber in the replacement of synthetic, non-biodegradable material [10]. Among various natural fibers such as pineapple, bamboo, sisal, hemp, coir, palm, banana, and abaca, the kenaf fiber is considered the world's important natural fiber, under denomination of "International Year of Natural Fibers 2009." The bast part of the kenaf plant constituents is nearly 40% of fiber; because of this, it is majorly utilized in most of the polymer

composite industry [11]. Further, due to their high tensile strength of 800 MPa, it is suitable to utilize as natural fiber in various engineering applications.

For example, Fajrin et al. [12] investigated the mechanical properties of kenaf fiber reinforced composite material. The authors resulted that the study shows that the addition of uni-directional kenaf fiber into the matrix shows maximum tensile, flexural properties of 76.5 MPa, and 151.3 MPa, respectively. Similarly, Muralidharan et al. [13] conducted a study on flammability, thermal stability properties of treated and untreated kenaf fiber reinforced polymer composite material. Author reported that kenaf fiber under silane treatment of 6% NaOH, resulted maximum thermal stability, flame retardant properties of material. Moreover, the kenaf fiber along with granite filler reinforced polymer composite and their behavior studied by Raja et al. [14]. In this author concluded that addition of kenaf fiber as significantly improves the tensile, flexural, impact, and hardness properties of composite material. Thus, due to their non-toxicity, renewability, high strength, and stiffness nature, the kenaf fiber was studied in a polymer composite field [15, 16]. Further, production of strong bonding adhesion and even load distribution of the composite is achieved by treating the fiber and filler under silane treatment condition [17].

Thus, from the above references, it is cleared that the potentiality of natural kenaf fiber reinforced composite has enhanced the mechanical and thermal properties of the material. Further, the addition of biomass extracted silane-treated crystalline cellulose particle could profoundly enhance the load carrying capacity of the material. Therefore, the present study investigates the silane-treated kenaf fiber and crystalline nanocellulose particle reinforced composite material and their mechanical, fatigue creep, and DMA behavior. In addition to these characteristics, the biodegradability, light weight, low cost, and eco-friendly nature of the biocomposite materials are utilized in automobile, aviation, space science, sports, and civil and marine engineering applications.

## 2 Experimental procedure

### 2.1 Material

In this study, the vinyl ester resin grade name (AY-9102) of density 1.05 g/cm<sup>3</sup> and viscosity of 350 cps was used along with catalyst, accelerators, and promoters to initiate the curing process of the matrix. These resin and other additives are purchased from Aypols Polymers Private Limited. Further, the natural kenaf fiber woven mat of density 0.75 g/cm<sup>3</sup> and aerial density of 320 GSM was procured from Metro Composite, Chennai, India. The silane treatment was carried out by using 3-aminopropyltriethoxysilane (CAS No:919–30-2), and it was supplied by Sigma-Aldrich, USA. For preparing

the crystalline nanocellulose particle from *Selenicereus undatus* (dragon fruit) outer cover waste biomass was purchased from fruits export traders, Chennai, India.

### 2.2 Crystalline nanocellulose preparation from *Selenicereus undatus*

The present paper study used crystalline nanocellulose as filler particle which were obtained from *Selenicereus undatus* (SU) fruit’s outer cover via alkaline pulping process (in this the alkaline solution is used to react with the hydrocarbons of plant based raw materials). First, the outer cover is removed from the fruit and washed thoroughly under distilled water and dried out under hot air oven at 80°C for

90 min, in order to remove the waste dust and moisture contaminants. Now, the dried SU fruit cover is grained well. The obtained grained powder of 10 g was mixed with 12 ml of 1 Mol of NaOH and 88 ml of distilled water solution, and it was continuously stirred under magnetic stirrer at 300 rpm for 2 h at 80°C. After being stirred, the obtained solution is filtered using Whatman filter paper grade 41. Following this delignification process, it is now allowed to dry out for 24 h at room temperature [18]. Now, these particles are bleached in a solution of 50 ml sodium hypochlorite (NaOCl) and 50 ml of distilled water and stirred again at 80°C for 1 h. It is a oxidation process and during this the dissolving sodium hypochlorite in water leads to the formation of the hypochlorous acid H C l O and the hypochlorite

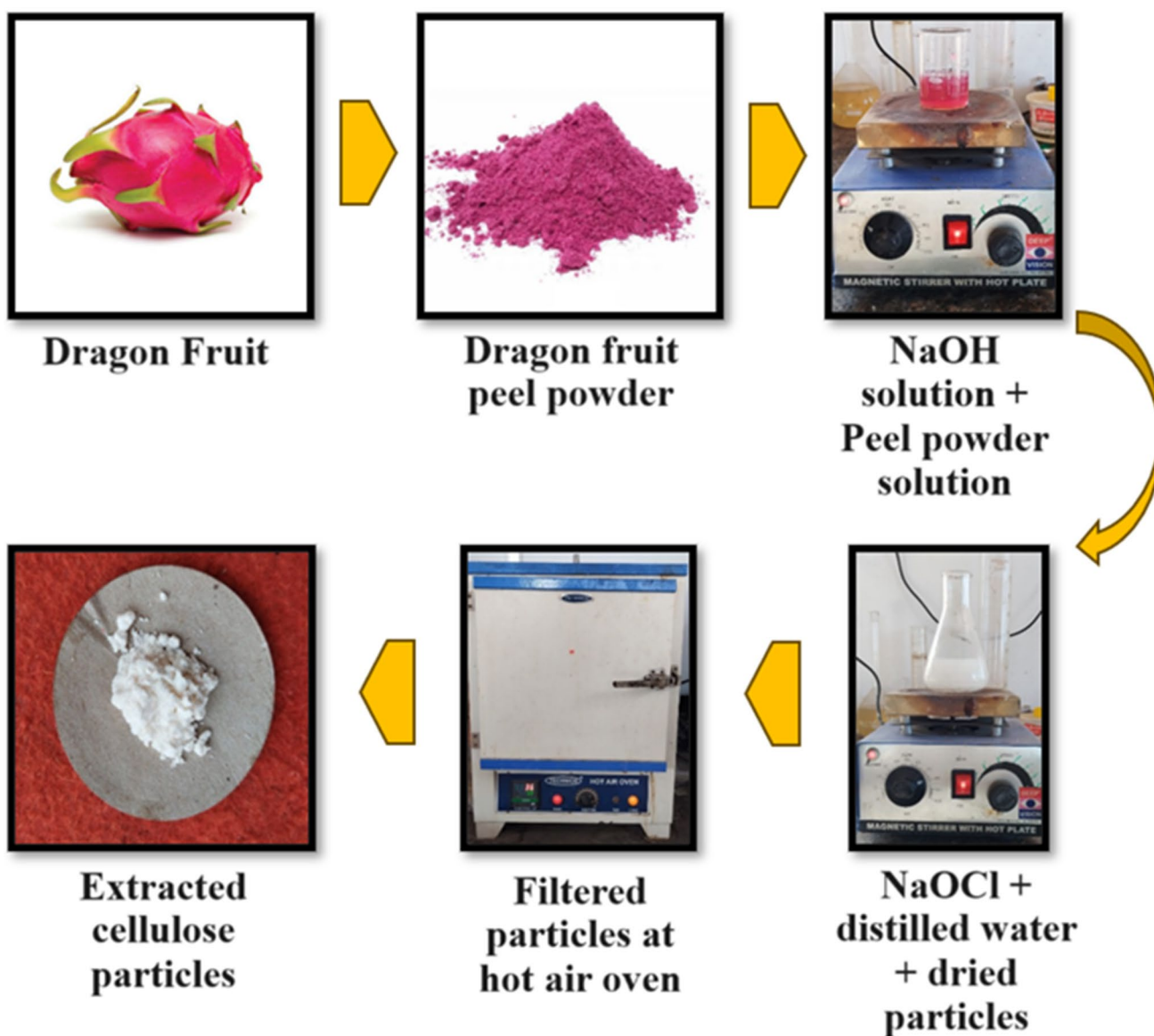
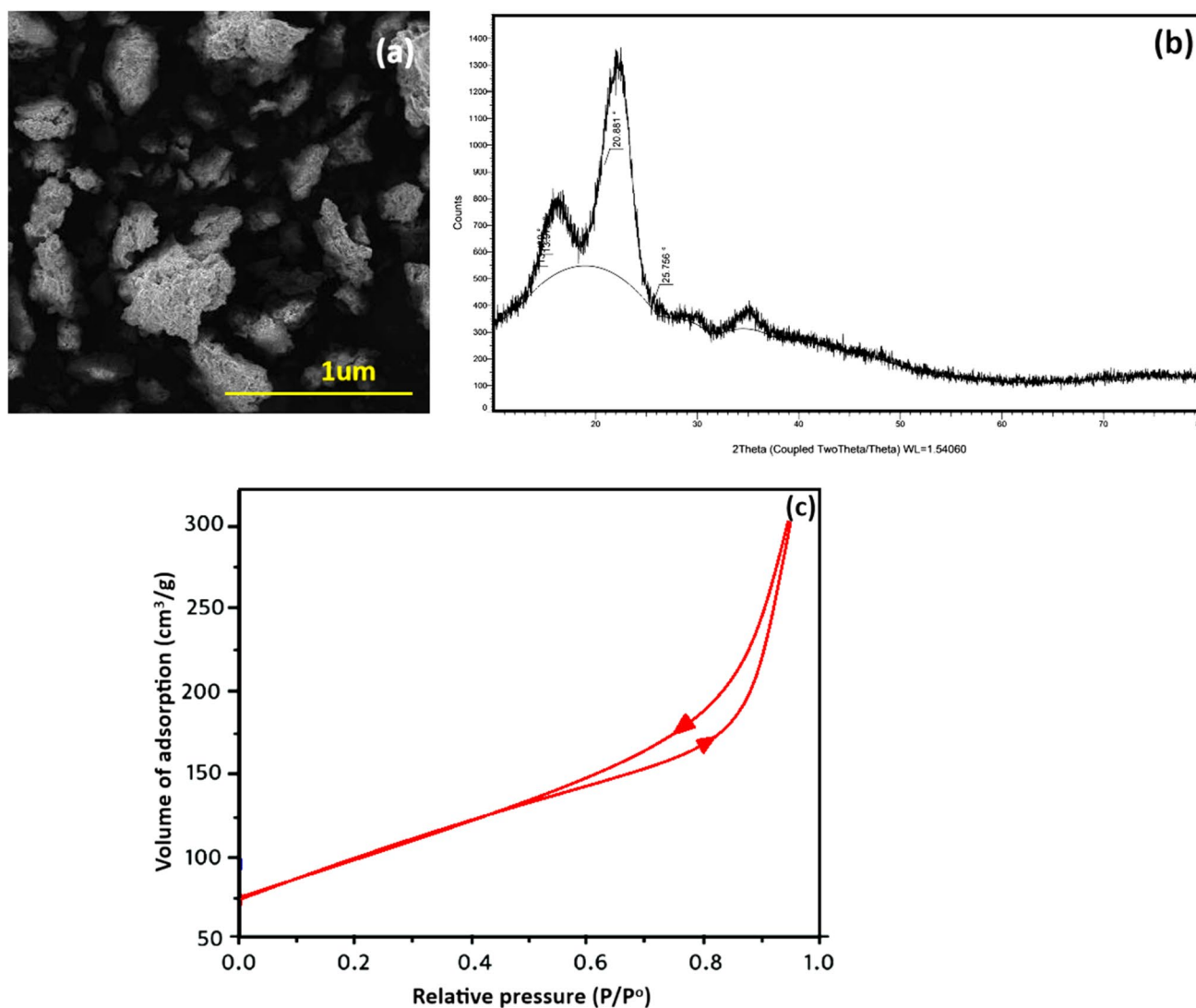


Fig. 1 preparation of crystalline nanocellulose from *Selenicereus undatus*



**Fig. 2** a FESEM, b XRD, and c BET analysis graphs of extracted nanocellulose from *Selenicereus undatus*

ions C 1 O – . The stirred particle is filtered under Whatman filter paper grade 41. Now these obtained cellulose particles are washed under distilled water for 3 h and kept in a hot air oven to neutralize the pH (pH = 7) of the particle. Finally, the particles are fine grained using ball mill for 20 min in order to obtain crystalline nanocellulose of size 200–400 nm with the purity of 98% (from XRD plot). The process flowchart for preparation of crystalline nanocellulose is mentioned in Fig. 1. Figure 2 shows the FESEM, XRD, and BET graph of extracted nanocellulose from *Selenicereus undatus*. The FESEM image (Fig. 2a) revealed that the nanocellulose is in submicron level with moderate size uniformity. Similarly, the XRD (Fig. 2b) shows two major peaks at 15.068° and 21.486° which indicate the presence of cellulose type 1, exhibiting monoclinic structure. Finally, the BET analysis shows the adsorption

and desorption curves of nanocellulose in N<sub>2</sub> gas flow. From the graph, it is observed that the BET surface area of the nanocellulose is 742 (m<sup>2</sup>g<sup>-1</sup>) with a pore volume of 0.86 (cm<sup>3</sup>g<sup>-1</sup>) and pore size of 26 nm.

### 2.3 Silane treatment

The silane treatment is imposed mainly to achieve strong mechanical and bonding strength between the matrix and reinforcement components; the natural fiber and the bio-filler reinforcement in both the fibers and fillers underwent a silane treatment process. Kenaf fiber and crystalline nanocellulose particles underwent a two-step silane treatment. Before starting the process, safety measures were undertaken such as using laboratory mask and gloves with apron to avoid hazardous accidents. The silane solution was first



**Fig. 3** FTIR spectra of silane-treated nanocellulose

**Table 1** Composite designation and with composition percentages

Composite designation	Vinyl ester resin (vol.%)	Kenaf fiber (vol.%)	Crystalline nanocellulose (vol.%)
V	60	40	–
VC0	59.5	40	0.5
VC1	59	40	1
VC2	58	40	2
VC3	56	40	4

V vinyl ester resin, C cellulose

made by combining 5% water and 95% ethanol. The pH of the mixture was then adjusted to a range of 4.5 to 5.5 using acetic acid. Moreover, the mixture was continuously agitated using a magnetic stirrer to guarantee the removal of methoxy groups and the full incorporation of silanol groups [19]. The silane was added to the solution gradually at a concentration of two weight percent until the required saturation level was reached. After immersing the fiber and filler particles in the silane solution for 10 min, the fiber and filler particles are heated to 110 °C for 20 min. The strength of the composite has been greatly increased by this silane treatment. Figure 3 shows the FTIR spectra of silane treated nanocellulose. The peak at 3408 cm<sup>-1</sup> indicates the presence of NH<sub>2</sub> functional group which is from the silane substance. Similarly, the peaks at 2924, 1635, and 1234.44 cm<sup>-1</sup> indicates the C-H stretch from the attached propyl group and the parent cellulose molecules. Similarly, a peak at 1041.56 cm<sup>-1</sup> indicates the C-N rock vibration from the primary cellulose polymeric chain to attached nitrogen and the asymmetrical stretch of

Si–O–Si structure which is the condensed silanol groups on the cellulose structure. Finally, the peak at 695.64 cm<sup>-1</sup> indicates the C–C rock from the primary cellulose. Thus, the FTIR study on silane-treated cellulose indicates that the silane grafting is effective and induced NH<sub>2</sub> functional groups on the cellulose structure, which could possibly react with resin during composite making process.

## 2.4 Development of composite

By using a hand layup technique [20], the crystalline nanocellulose from *Selenicereus undatus* fruit cover and kenaf fiber reinforced vinyl ester composite was prepared. This method was chosen due to its simplicity, versatility, and cost-effectiveness. Additionally, it requires minimal equipment and is suitable for small-scale production or prototyping. Initially, the vinyl ester resin was mixed with crystalline nanocellulose at various vol.% is mentioned in Table 1. This mixture was stirred under ultra-sonicate in order to obtain homogeneous solution. Before pouring this homogenous solution matrix into the mold, molten wax was applied to get smooth finished surface. Now, the resin mixture was added into the catalyst to further initiating the curing process. For 100 ml of vinyl ester resin, 1 ml of catalyst was used to initiate the curing process. Overall, 250 ml of resin was used for each designation composite plate. After placing the natural kenaf fiber mat (overall 3 layers of fibers with 0° orientation was involved) into the mold (30 cm long and wide), the resin was applied layer by layer of those fibers. By using a cotton roller, the excess resin was scrapped off, to avoid void formation. Now, it is allowed to cure in a ambient temperature for 24 h. After curing process, further the composite plate



**Fig. 4** Fabricated kenaf fiber and nanocellulose reinforced composite material

was subjected to post curing in a hot air furnace for 4 h at 110 °C. The prepared composite and their designation are represented in Fig. 4.

### 3 Characterization of composites

Once the post curing of the crystalline nanocellulose and natural fiber reinforced composite, it allowed testing for analyzing their performance. The performance of the composite is analyzed by testing the specimen under ASTM standard. Thus, as per ASTM standard, the testing such as tensile, flexural, ILSS, impact, hardness, fatigue, creep, and DMA was carried out by cutting under abrasive water jet machine (Maxieum, 1515 KENT, USA). The abrasive water jet machine operates with a water impinging pressure

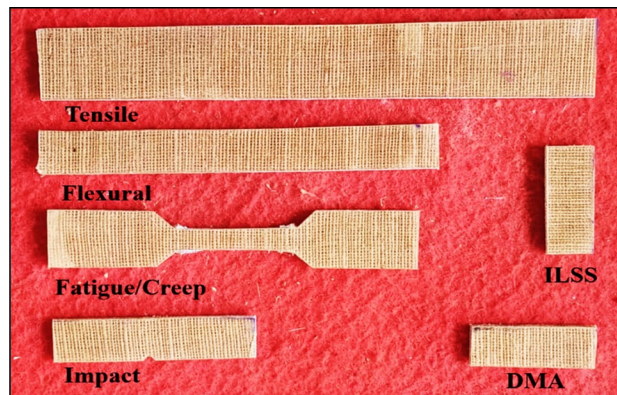


**Fig. 5** Testing specimen of kenaf fiber and nanocellulose particle reinforced composite material

of 170 psi, particle size of 10 to 30 microns, and standard deviation of 0.3 which were used as process variables. To achieve well-finished specimens, a nozzle with a diameter of 0.3 mm was employed. The testing ASTMs and machine specification are mentioned in Table 2, respectively. Overall, five specimens were prepared for each test conducted as indicated in Table 2. Test specimens as per ASTM standards are shown in Fig. 5.

## 4 Results and discussion

### 4.1 Mechanical properties

Figure 6a–e illustrates the mechanical attributes of various composite formulations denoted as V, VC0, VC1, VC2, and VC3. Initially labeled as V, this composite demonstrates respectable mechanical properties including a tensile

**Table 2** ASTM standard testing and their machine specification

Test	ASTM	Dimensions	Machine specification	Reference
Tensile	D 3039	Wide—25 mm, long—250 mm	Testing was done under Universal Testing Machine. Instron 4855, UK.	[21]
Flexural	D 790	Wide—13 mm, long—125 mm	Machine run at a traverse speed of 1.5 mm/min	[22]
ILSS	D 2344	Wide—8 mm, long—50 mm		[23]
Izod impact	D 256	Wide—12.7 mm, long—63.5 mm	Krystal equipment, India. Impact test will assess energy absorbed by a material during fracture. Maximum load capacity of 20 J	[24]
Hardness	D 2240	Wide—15 mm, long—35 mm	Surface hardness of the composite material is assessed by under Mitutoyo, shore-D. Blue steel, India	[25]
Fatigue	D 3479	Wide—25 mm, long—250 mm	Tension-tension fatigue machine MTS, Bionic landmark 370, USA was used. Load is applied of 25%, 50%, and 70% of UTS, stress ratio of 0.1, R value of -1, tensile modulus of 6 GPa, and frequency of 5 Hz	[26]
Creep	D 7337	Wide—12.7 mm, long—127 mm	Metro precision machine tools India, Private Ltd. Load of 30% UTS, time of 15000 s and temperature of 50°C was set as process variables	[27]
DMA	D 4065	Wide—12.8, long—50 mm	SEIKO, DMS EXSTAR 6100, USA. Dual cantilever, sweep mode was followed with 1-Hz frequency	[28]

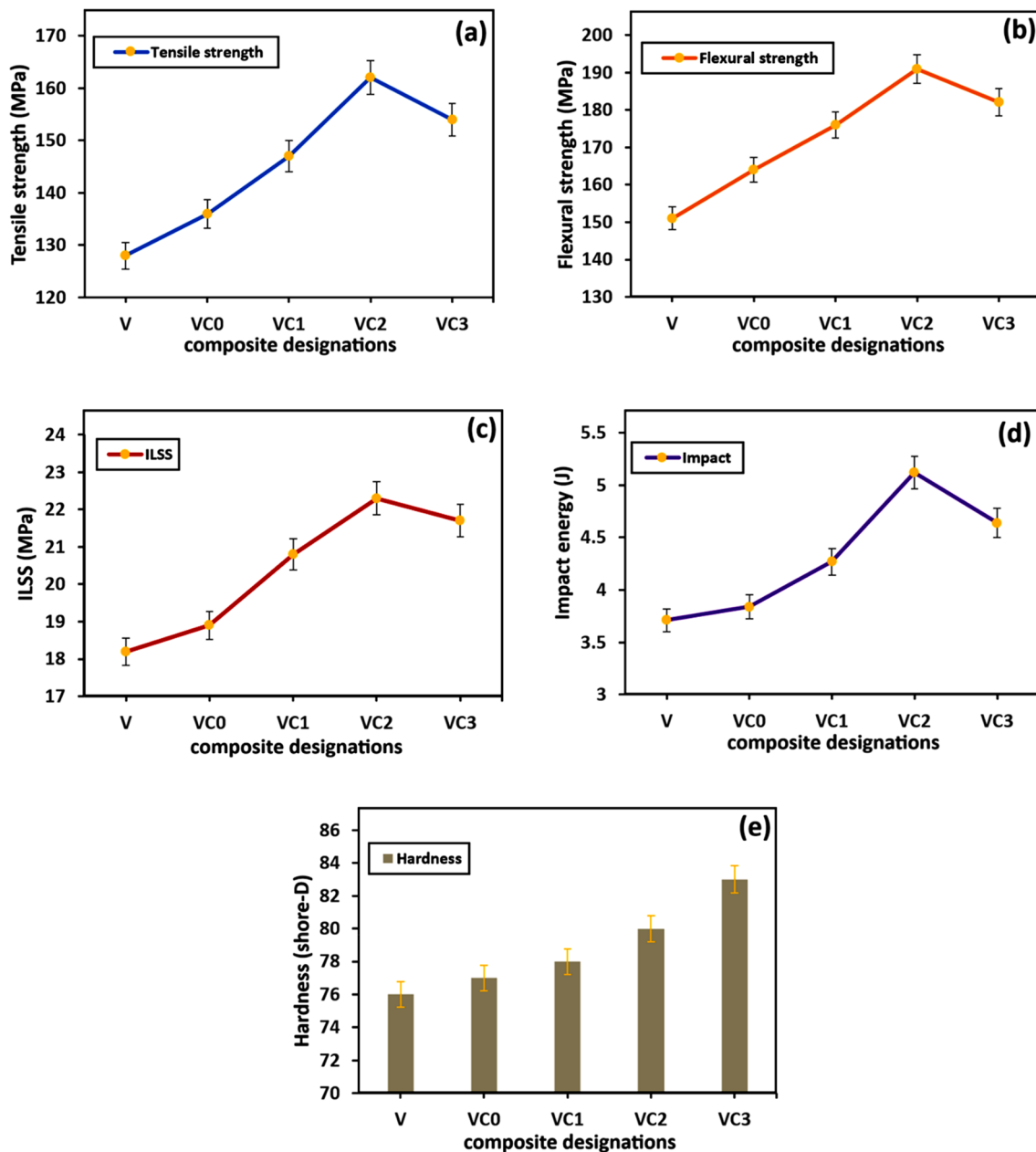


**Fig. 6** Mechanical properties, **a** tensile strength, **b** flexural strength, **c** interlaminar shear strength, **d** impact energy, and **e** hardness of different composite designations

strength of 128 MPa, flexural strength of 151 MPa, interlaminar shear strength (ILSS) of 18.2 MPa, impact energy of 3.71 J, and a hardness of 76 Shore-D. The commendable strength of the matrix can be attributed to the presence of kenaf fibers, which confer stiffness to the vinyl ester matrix, effectively reinforcing the structure and enhancing load distribution [29].

However, by incorporating nanocellulose particles at various volumes (0.5%, 1%, 2%, and 4%) alongside 40% volume of kenaf fibers, the mechanical properties of the composites

are significantly augmented, resulting in improved characteristics for VC0, VC1, VC2, and VC3. Particularly noteworthy is VC2, which exhibits the highest mechanical properties among the composite designations, boasting a tensile strength of 162 MPa, flexural strength of 191 MPa, ILSS of 22.3 MPa, impact energy of 5.12 J, and a hardness of 80. Compared to the base composite V, VC2 demonstrates a remarkable increase of 20.98% in tensile strength, 21.3% in flexural strength, 18.3% in ILSS, and 27.3% in impact energy. This enhancement is primarily attributed to the

presence of nanoscale cellulose, which enhances the interfacial adhesion between kenaf fibers and the matrix. The diminutive dimensions of cellulose particles facilitate superior integration, resulting in enhanced stress transfer and overall mechanical performance [30]. Additionally, silane treatment of kenaf fiber and nanocellulose filler contributes to their uniform dispersion and enhanced adhesion within the matrix [31].

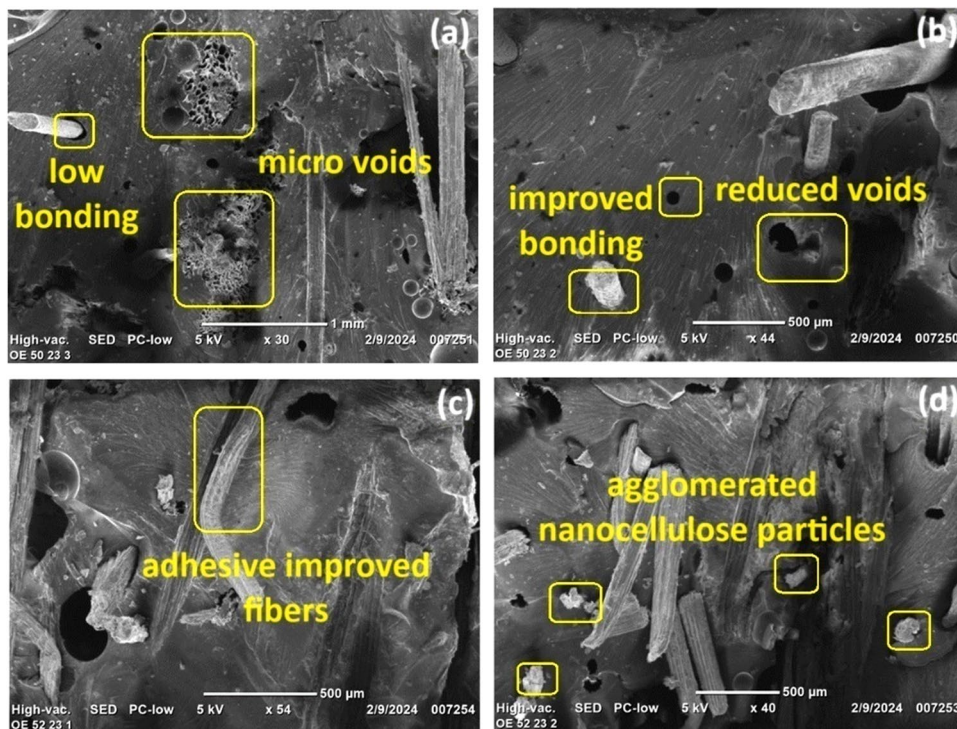
On the contrary, VC3 experiences a slight decrement in mechanical properties, with a tensile strength of 154 MPa, flexural strength of 182 MPa, ILSS of 21.7 MPa, and impact energy of 4.64 J. Compared to VC2, VC3 demonstrates a reduction of 4.9% in tensile strength, 4.7% in flexural strength, 2.6% in ILSS, and 9.3% in impact energy. This decline is attributed to the agglomeration of cellulose particles within the matrix due to their higher concentration [32], leading to the formation of stress concentration points that result in breakage under load [33]. Nonetheless, the heightened concentration of nanocellulose in VC3 enhances the rigidity of the matrix, resulting in increased hardness (83). However, this heightened rigidity compromises flexibility, impacting the material's ability to deform and absorb energy. Nevertheless, VC3 still outperforms the base composite V in terms of mechanical properties.

Figure 7a–d displays scanning electron microscope (SEM) images of fractured tensile specimens for V, VC0, VC1, and VC3, respectively. In Fig. 7a, micro voids are evident in the matrix, contributing to diminished mechanical

properties. Additionally, there is a noticeable lack of strong bonding between the kenaf fiber and the vinyl ester matrix in this image, moving to Fig. 7b, due the presence of nanocellulose particles in the matrix results in reduced voids and improved bonding with kenaf fibers [34]. This improvement is correlated with enhanced mechanical properties, indicating that the addition of nanocellulose has a positive impact on the structural integrity of the composite material. Figure 7c reveals even more enhanced adhesion in the matrix with the further addition of nanocellulose. Voids are significantly reduced, leading to improved structural integrity and reinforcing the positive effects on mechanical properties.

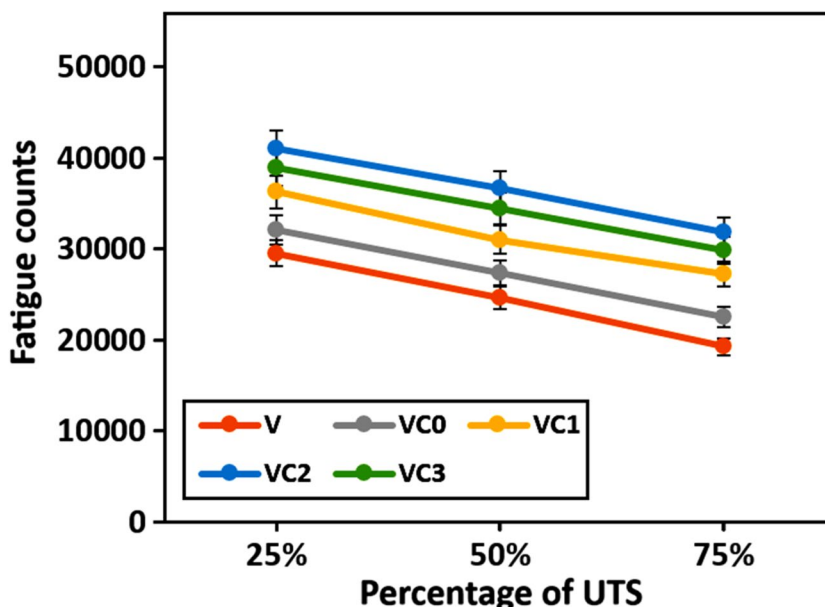
However, in Fig. 7d, which corresponds to the inclusion of a high-volume percentage of nanocellulose in VC3, agglomeration of nanocellulose particles is observed. This agglomeration creates stress concentration points in the matrix, ultimately resulting in reduced mechanical properties. The clustered particles form areas of weakness, leading to compromised structural integrity. In overall, the SEM images illustrate the correlation between microstructural features and mechanical properties. The progression from micro voids and weak bonding in V to reduced voids and enhanced bonding in VC1 indicates the positive impact of nanocellulose. Nevertheless, the agglomeration observed in VC3 emphasizes the importance of optimizing the volume percentage of nanocellulose to avoid detrimental effects on the mechanical performance of the composite material.

**Fig. 7** SEM images of fractured tensile specimens





**Fig. 8** Fatigue counts of different composite designations



**4.2 Fatigue properties**

Figure 8 illustrates the fatigue counts associated with various composite designations, including V, VC0, VC1, VC2, and VC3. A fatigue test was conducted to evaluate the material’s performance over multiple cyclic periods. This test aimed to assess how the material behaved under repeated loading and unloading cycles, providing insights into its endurance and durability over time. The V composite designation exhibits fatigue counts of 29,554, 24,643, and 19,271 for 25%, 50%, and 75% of the ultimate tensile strength (UTS). The presence of kenaf fibers in the matrix contributes to improved stress distribution within the composite, offering additional pathways for stress dissipation and reducing the risk of localized stress concentrations that might lead to fatigue failure [35]. Furthermore, the addition of nanocellulose particles at different volume percentages (0.5, 1, 2, 4) along with kenaf fibers enhances fatigue counts in VC0, VC1, VC2, and VC3. VC2, in particular, demonstrates the highest fatigue counts

of 40,982, 36,712, and 31,854 for 25%, 50%, and 75% of UTS, respectively. Compared to V, VC2 shows significant improvements of 27.8%, 32.8%, and 39.5% for the corresponding UTS percentages. The nanocellulose within the vinyl ester matrix, with its nanoscale dimensions, improves interaction with kenaf fibers and the matrix, enhancing adhesion at the interface [36]. This improved adhesion facilitates better load transfer between the matrix and the fibers, potentially mitigating the initiation and propagation of fatigue-induced cracks.

However, as the content of nanocellulose in the matrix increases, fatigue counts decrease. VC3, with higher nanocellulose content, delivers reduced fatigue counts of 38,939, 34,490, and 29,907 for 25%, 50%, and 75% of UTS. This reduction is attributed to the increased rigidity resulting from higher nanocellulose content in the matrix [37]. The heightened rigidity, while providing enhanced hardness, can limit flexibility and increase susceptibility to fatigue damage during cyclic loading [38]. Nonetheless, the observed

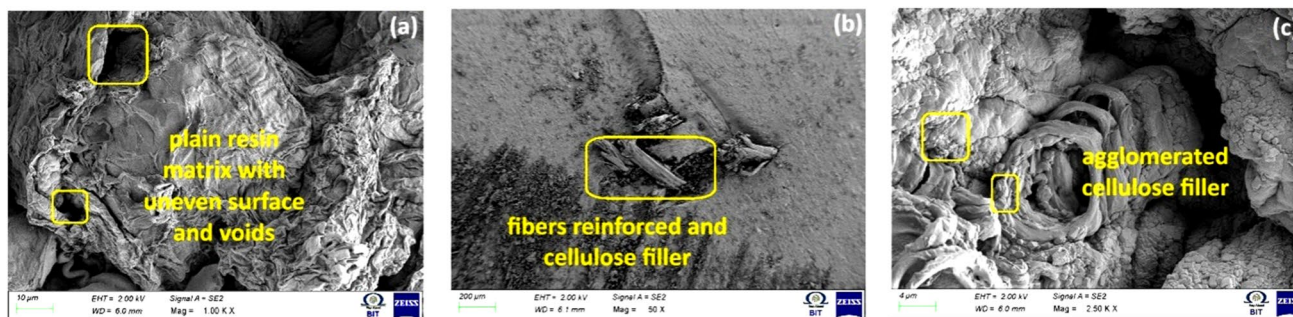


**Fig. 9** SEM images of fatigue specimens

reduction in fatigue counts for VC3 is relatively slight, and the fatigue performance remains better than that of the V composite designation. VC2's fatigue properties indicate its ability to withstand cyclic loading environments, making it suitable for applications in aerospace, automotive, sports equipment, marine structures, and infrastructure projects. Its resilience under repetitive stress conditions promises extended service life and enhanced safety across diverse industries.

The images in Fig. 9 illustrate the SEM (Scanning Electron Microscopy) views of fractured fatigue test specimens. In Fig. 9a, the plain matrix is depicted, revealing the presence of voids and the formation of cracks. These imperfections significantly diminish the material's fatigue strength under cyclic loading conditions. Moving to Fig. 8b, it showcases the incorporation of kenaf fiber reinforcement with cellulose filler. This addition facilitates superior bonding within the matrix, consequently mitigating the adverse effects of cyclic loads. As a result, the fatigue strength of the material is notably enhanced compared to the plain matrix observed in Fig. 9b. Figure 9c provides insight into the impact of cellulose fillers at higher volume percentages. Here, clusters of

cellulose fillers are evident. However, instead of enhancing the material's fatigue resistance, these clusters create stress points within the matrix. Consequently, the formation of stress points leads to a reduction in fatigue counts, indicating a decline in fatigue strength. In summary, the SEM images in Fig. 8 highlight the influence of different reinforcements and fillers on the fatigue behavior of the material. While kenaf fiber reinforcement with cellulose filler improves fatigue strength by promoting better bonding, excessive clustering of cellulose fillers at higher volume percentages adversely affects fatigue performance by creating stress concentrations within the matrix. Table 3 shows the quantitative comparison and percentage of improvement between composites.

### 4.3 Creep behavior

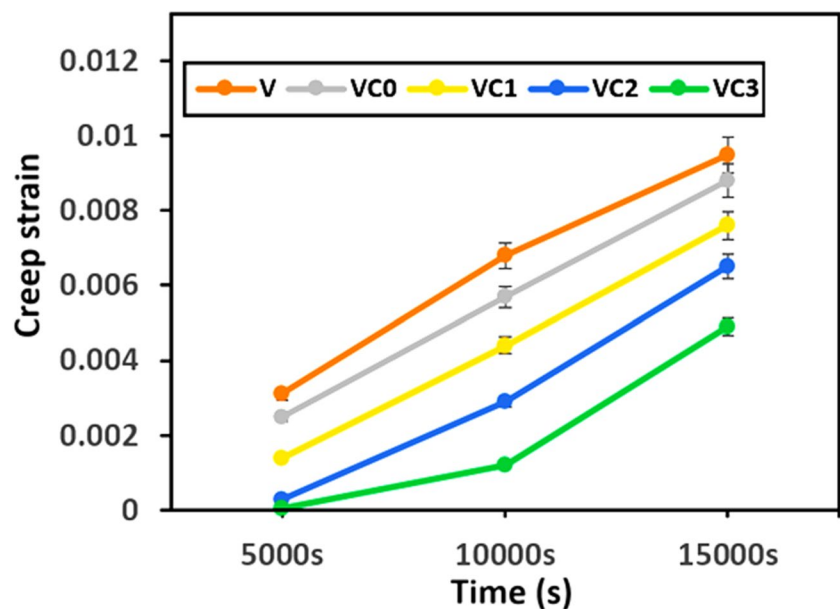
Figure 10 provides an overview of the creep strain exhibited by various composite designations, namely V, VC0, VC1, VC2, and VC3. In the case of the V composite designation, the recorded creep strain values are 0.0031, 0.0068, and 0.0095 for time intervals of 5000 s, 10,000 s, and 15,000 s, respectively. This indicates that the incorporation of kenaf fibers enhances the dimensional stability of the composite material. The presence of these fibers helps restrict matrix movement, reducing the material's susceptibility to deformation under sustained stress and temperature conditions [39]. The inclusion of nanocellulose in the matrix, in conjunction with kenaf fibers, leads to further reductions in creep strain [40], as observed in VC0, VC1, VC2, and VC3.

Consequently, an increased volume of nanocellulose corresponds to a decreased creep strain. Specifically, the VC3 composite designation exhibits the lowest creep strain values of 0.00053, 0.0012, and 0.0049 for the respective time

**Table 3** Quantitative comparison and percentage of improvement

Composite designations	Percentage of increase in counts compared with V		
	25% UTS	50% UTS	75% UTS
VC0	7.95	10	14.35
VC1	18.53	20.52	29.2
VC2	27.88	32.87	39.5
VC3	24.1	28.5	35.5

**Fig. 10** Creep strain of different composite designations



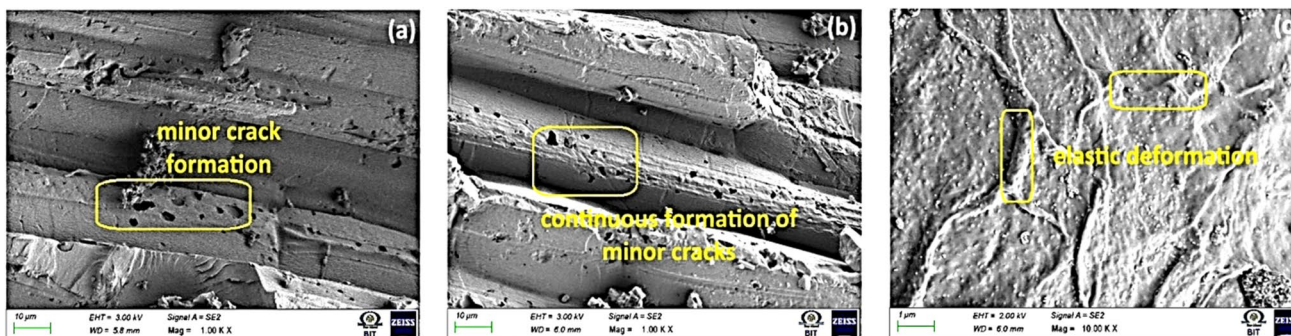


Fig. 11 SEM images of creep test specimens

intervals. This emphasizes that the presence of nanocellulose, when combined with kenaf fiber, significantly contributes to the improved dimensional stability of the composite material. The nanoscale dimensions of cellulose particles play a crucial role in filling void gaps within the matrix and enhancing packing efficiency [41]. This, in turn, restricts the movement of polymer chains, minimizing the propensity for the material to undergo creep. The collaborative effects of kenaf fibers and nanocellulose contribute to a composite material with enhanced resistance to deformation over extended time periods, making it well-suited for applications where dimensional stability is a critical consideration.

Figure 11 presents SEM images capturing the outer surface of specimens subjected to creep testing. In Fig. 11a, b, one can observe the emergence of minor cracks resulting from the consistent load applied to the specimens. Moreover, continuous crack formation is evident on the surface, indicative of the sustained stress experienced during the testing process. Figure 11c illustrates the phenomenon of elastic deformation observed on the surface due to the application

of load at elevated temperatures over a certain duration. This deformation is a consequence of the material’s response to the combination of elevated temperature and applied load, resulting in observable changes in its surface morphology. Overall, the SEM images in Fig. 10 provide valuable insights into the effects of creep testing on the surface characteristics of the specimens. The observed crack formation and elastic deformation underscore the material’s response to prolonged stress and elevated temperatures, highlighting crucial considerations for understanding its creep behavior. However based on the results obtained, the creep test could be conducted with higher temperature and duration in order to know the sever deformation on the real time products when they are exposed to temperature and water.

#### 4.4 DMA analysis

Figure 12a, b presents the dynamic mechanical analysis (DMA) characteristics, including storage modulus and loss factor, for different composite designs. In the case of the

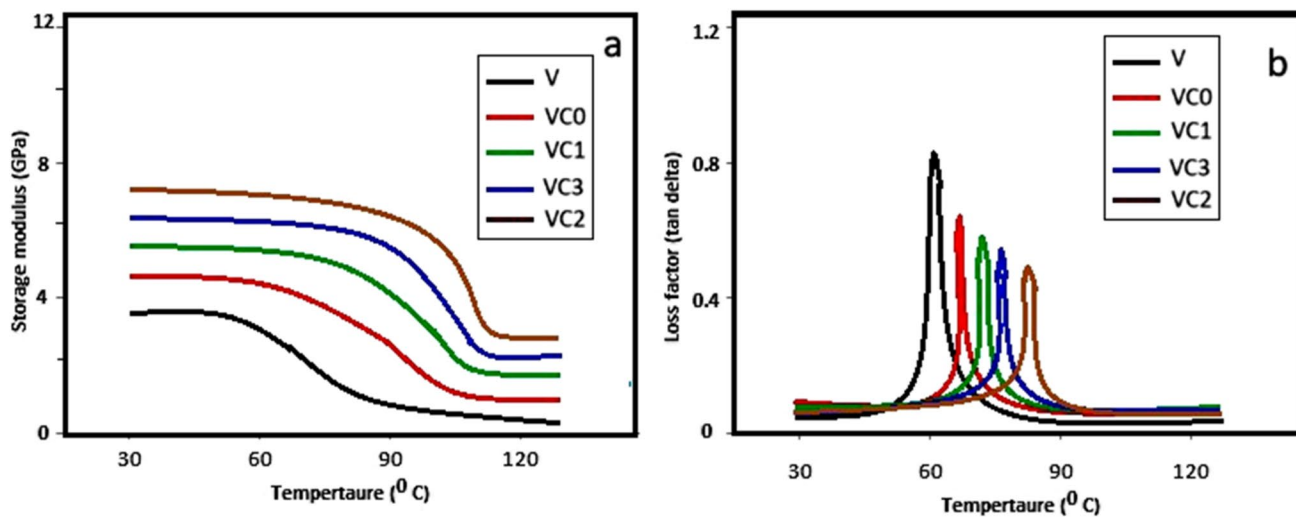


Fig. 12 DMA characteristics, a storage modulus and b loss factor, of different composite designs

V composite designation, a storage modulus of 3.8 GPa and a loss factor of 0.83 are observed. These values are attributed to the presence of kenaf fibers, which facilitate stress distribution uniformly within the material [42]. This effective load distribution contributes to an enhanced storage modulus by minimizing localized stress concentrations and improving overall structural integrity. Upon further inclusion of nanocellulose with kenaf fiber, the storage modulus is boosted. Consequently, VC0, VC1, VC2, and VC3 exhibit storage moduli of 3.8 GPa, 4.6 GPa, 6.8 GPa, and 6.1 GPa, respectively, with corresponding loss factor values of 0.69, 0.6, 0.46, and 0.58.

Notably, VC3 shows a slight reduction in storage modulus coupled with a slight increment in the loss factor, making VC2 the designation with the highest storage modulus. The observed enhancement in storage modulus is attributed to the improved interaction between kenaf fibers and the matrix facilitated by nanocellulose particles [43]. This enhanced adhesion at the interface results in better load transfer and stress distribution within the composite material. The synergistic effects of nanocellulose and kenaf fibers lead to an improved storage modulus and reduced loss factor. However, the observed slight reduction in VC3 is associated with the higher volume of nanocellulose. Achieving uniform dispersion of nanocellulose throughout the matrix becomes challenging at elevated volumes [44], even with silane treatment. Poor dispersion leads to uneven distribution and agglomeration of particles [45], ultimately contributing to the reduced storage modulus in the VC3 designation.

## 5 Conclusions

In conclusion, this research delved into the synthesis and integration of nanocellulose from *Selenicereus undatus* into kenaf fiber-reinforced Vinyl Ester composites. Among the arrays of formulations, VC2 emerged as a standout performer, demonstrating remarkable mechanical strength with a tensile strength of 162 MPa, flexural strength of 191 MPa, ILSS of 22.3 MPa, impact energy absorption of 5.12 J, and a hardness of 80. Due to increased rigidity with higher volume of nanocellulose, VC3 delivers higher shore-D hardness of 83. Additionally, VC3 showcased exceptional fatigue endurance, exhibiting fatigue counts of 40,982, 36,712, and 31,854 for 25%, 50%, and 75% of the ultimate tensile strength (UTS), indicative of robust cyclic loading performance. Notably, VC4 demonstrated reduced creep strain values of 0.0052, 0.0012, and 0.0049 for time intervals of 5000 s, 10,000 s, and 15,000 s, showcasing the material's resistance to deformation over extended periods. In terms of dynamic mechanical properties, VC2 exhibited an impressive storage modulus of 6.8 GPa, coupled with a reduced loss factor of 0.46, highlighting efficient energy storage and reduced dissipation during cyclic loading. Collectively, these

results underscore the superior performance of the VC2 composite across various mechanical and dynamic properties. Overall, the utilization of filler derived from *Selenicereus undatus* yielded superior reinforcement for the matrix. Moreover, incorporating a natural source enhances the environmentally friendly aspect of the material. This emphasizes the efficacy of incorporating nanocellulose-reinforced kenaf fiber and vinyl ester composites for diverse applications.

## 6 Future research direction

Future research needs to delve into exploring filler content and its variability. The current study has encountered issues with cluster and agglomeration formation when filler content is high. The forthcoming investigations aim to mitigate the effects of clustering and minimize filler agglomeration. Similarly, researchers will explore the combination of extracted fillers with various fibers to assess the resulting variations. Moreover, since this biocomposite has essential properties to be acts as structural material for automotives, the auto industries could come forward to make automobile pumps, roof panel, and door inside panel using this material.

**Acknowledgements** The authors express gratitude to the management for their provision of resources and assistance enabling the completion of this research.

**Author contribution** R. Ashok Raj and K. Vinoth Kumar: full research. Rajkumar Subburathinam and H. Vinoth Kumar: testing support.

**Data availability** All data are available within the manuscript. No more additional data is available.

## Declarations

**Ethics approval** Not applicable.

**Competing interests** The authors declare no competing interests.

## References

1. Syduzzaman MD et al (2023) Results in materials 100448. <https://doi.org/10.1016/j.rinma.2023.100448>
2. Karaoui M, Hsissou R, Alami M, Assouag M (2023) Iran Polym J 32(5):621–631. <https://doi.org/10.1007/s13726-023-01151-2>
3. Kumar P, Kumar M, Roopa CP (2022) J Indian Chem Soc 99(10):100715. <https://doi.org/10.1016/j.jics.2022.100715>
4. Fahma F, Febiyanti I, Lisdayana N, Arnata IW, Sartika D (2021) Arch Mater Sci Eng 109(2):49–64. <https://doi.org/10.5604/01.3001.0015.2624>
5. Tien NNT, Le NL, Khoi TT, Richel A (2022) Biomass Conversion Biorefinery. 1–13. <https://doi.org/10.1007/s13399-021-02146-w>
6. Kaur P, Sharma N, Munagala M, Rajkhowa R, Aallardyce B, Shastri Y, Agrawal R (2021) Front Nanotechnol 3:747329. <https://doi.org/10.3389/fnano.2021.747329>

7. Bosenbecker MW, Cholant GM, Silva GEHD, Paniz OG, Carreño NLV, Marini J, Oliveira ADD (2020) *Polímeros* 29:e2019058. <https://doi.org/10.1590/0104-1428.04819>
8. Sunesh NP, Indran S, Divya D, Suchart S (2022) *Polym Compos* 43(9):6476–6488. <https://doi.org/10.1002/pc.26960>
9. Nagarajan KJ, Balaji AN, Basha KS, Ramanujam NR, Kumar RA (2020) *Int J Biol Macromol* 152:327–339. <https://doi.org/10.1016/j.ijbiomac.2020.02.255>
10. Mohammed M, Jawad AJAM, Mohammed AM, Olewi JK, Adam T, Osman AF, ... Jaafar M (2023) *Polymer Testing*. 108083. <https://doi.org/10.1016/j.polymertesting.2023.108083>
11. Bhanuprakash L, Manikandan N, Raphel A, Mangalathu GS (2023). *Mater Today Proc*. <https://doi.org/10.1016/j.matpr.2023.06.247>
12. Fajrin J, Akmaluddin A, Gapsari F (2022) *Results Eng* 13:100380. <https://doi.org/10.1016/j.rineng.2022.100380>
13. Muralidharan ND, Subramanian J, Rajamanickam SK, Gopalan V (2023) *J Polym Eng* 43(10):865–874. <https://doi.org/10.1515/polyeng-2023-0128>
14. Raja T, Mohanavel V, Kumar SS, Rajkumar S, Ravichandran M, Subbiah R (2022) *Mater Today Proc* 59:1345–1348. <https://doi.org/10.1016/j.matpr.2021.11.548>
15. Uzoma AE, Nwaeche CF, Al-Amin M, Muniru OS, Olatunji O, Nzeh SO (2023) *Eng* 4(2):1698–1710. <https://doi.org/10.3390/eng4020096>
16. Arjmandi R, Yıldırım I, Hatton F, Hassan A, Jefferies C, Mohamad Z, Othman N (2021) *J Eng Fibers Fabr* 16:15589250211040184. <https://doi.org/10.1177/15589250211040184>
17. Hosseini SB, Gaff M, Li H, Hui D (2023) *Rev Adv Mater Sci* 62(1):20230131. <https://doi.org/10.1515/rams-2023-0131>
18. Bhardwaj S, Singh S, Meda RS, Jain S, Maji PK (2023) *Biomass Convers Biorefinery*. 1–14. <https://doi.org/10.1007/s13399-023-03970-y>
19. Sivakumar V, Kaliappan S, Natrayan L, Patil PP (2023) *Silicon* 1–9. <https://doi.org/10.1007/s12633-023-02370-1>
20. Venkatesh R, Ballal S, Krishnan AM, Prabakaran S, Mohankumar S, Ramaraj E (2023) *Heliyon* 9(5). <https://doi.org/10.1016/j.heliyon.2023.e15934>
21. Pinnell M, Fields R, Zabora R (2005) *J Test Eval* 33(1):27–31. <https://doi.org/10.1520/JTE12521>
22. Prasad MM, Harikrishnan R, Khan MS, Santhoshkumar T, Rajkumar T, Nandhagopan S (2023) *Mater Today Proc* 77:509–514. <https://doi.org/10.1016/j.matpr.2022.11.354>
23. Kumar S, Sharma N, Biswas R, Singh KK (2023). *Mater Today Proc*. <https://doi.org/10.1016/j.matpr.2023.03.327>
24. Bachi Al-Fahad IO, Hassan AD, Faisal BM, Sharaf HK (2023) *East-Eur J Enterp Technol* 124(7). <https://doi.org/10.15587/1729-4061.2023.286541>
25. Tavadi AR, Nagabhushana N, Vivek Bhandarkar VN, Jagadeesha T, Kerur MR, Rudresha S, ... Mohan DG (2024) *Arab J Sci Eng* 49(2):2311–2325. <https://doi.org/10.1007/s13369-023-08207-8>
26. Sharma N, Singh KK, Ansari MTA (2023). *Mater Today Proc*. <https://doi.org/10.1016/j.matpr.2023.05.357>
27. Mohamed K, Hassanein A, Benmokrane B (2023) In *International Symposium of the International Federation for Structural Concrete* (pp. 778–787). Cham: Springer Nature Switzerland. [https://doi.org/10.1007/978-3-031-32519-9\\_76](https://doi.org/10.1007/978-3-031-32519-9_76)
28. Kaushik D, Gairola S, Varikkadinmel B, Singh I (2023) *Polym Compos* 44(1):515–523. <https://doi.org/10.1002/pc.27114>
29. Abbas AGN, Aziz FNAA, Abdan K, Nasir NAM, Huseien GF (2023) *Constr Build Mater* 396:132160. <https://doi.org/10.1016/j.conbuildmat.2023.132160>
30. Marcuello C, Chabbert B, Berzin F, Bercu NB, Molinari M, Aguié-Béghin V (2023) *Materials* 16(6):2440. <https://doi.org/10.3390/ma16062440>
31. Li C, Liao H, Gao H, Cheng F (2024) Enhancing interface compatibility in high-filled coal gangue/polyethylene composites through silane coupling agent-mediated interface modification. *Compos Sci Technol* 110546. <https://doi.org/10.1016/j.compscitech.2024.110546>
32. James A, Rahman MR, Mohamad Said KA, Kanakaraju D, Sueraya AZ, Kuok KK, ... Rahman MM (2023) *J Thermoplast Compos Mater* 08927057231205451. <https://doi.org/10.1177/08927057231205451>
33. Khan K, Johari MAM, Amin MN, Iqbal M (2024) *Case Stud Constr Mater* 20:e02699. <https://doi.org/10.1016/j.cscm.2023.e02699>
34. Seydibeyoğlu MÖ, Dogru A, Wang J, Rencheck M, Han Y, Wang L, ... Gardner DJ (2023) Review on hybrid reinforced polymer matrix composites with nanocellulose, nanomaterials, and other fibers. *Polymers* 15(4):984. <https://doi.org/10.3390/polym15040984>
35. Khan A, Sapuan SM, Siddiqui VU, Zainudin ES, Zuhri MYM, Harussani MM (2023) *Int J Biol Macromol* 127119. <https://doi.org/10.1016/j.ijbiomac.2023.127119>
36. Ni K, Du G, Liu C, Wu Y, Yang H, Yin C, ... Yang L (2023) Cross-linked entanglement of aldehyde and amine-functionalized nanocellulose reinforced with biomimetalization to produce an all-bio-based adhesive. *Chem Eng J* 465:142888. <https://doi.org/10.1016/j.cej.2023.142888>
37. Dias IK, Lacerda BK, Arantes V (2023) *Int J Biol Macromol* 242:125053. <https://doi.org/10.1016/j.ijbiomac.2023.125053>
38. Zhao LC, Xu L, Yazdi A (2023) Laboratory evaluation of the effect of waste materials on mechanical properties of asphalt binder and mixture containing combined natural binder and waste polymer. *Constr Build Mater* 403:132995. <https://doi.org/10.1016/j.conbuildmat.2023.132995>
39. Oliver BA, Dong Q, Ramezani M, Selles MA, Sanchez-Caballero S (2023) Tribological performance of bamboo fabric reinforced epoxy composites. *Macromol Mater Eng* 308(9):2300077. <https://doi.org/10.1002/mame.202300077>
40. Neves RM, Ornaghi Jr HL, Alves FC, Zattera AJ, Tom M, Lal HM, ... Thomas S (2023) Creep and stress relaxation behavior of functionalized microcrystalline cellulose/epoxy composites. *Cellulose*, 30(4), 2197–2216. Neves, R. M., Ornaghi Jr, H. L., Alves, F. C., Zattera, A. J., Tom, M., Lal, H. M., ... & Thomas, S. (2023). Creep and stress relaxation behavior of functionalized microcrystalline cellulose/epoxy composites. *Cellulose* 30(4):2197–2216
41. Tang S, Wu Z, Li X, Xie F, Ye D, Ruiz-Hitzky E, ... Wang X (2023) *Carbohydr Polym* 299:120204. <https://doi.org/10.1016/j.carbpol.2022.120204>
42. Mohapatra DK, Deo CR, Mishra P, Ekka KK, Mishra C (2023) *Proc Inst Mech Eng Part E J Process Mech Eng* 237(6):2440–2448. <https://doi.org/10.1177/09544089221136813>
43. Zhao X, Bhagia S, Gomez-Maldonado D, Tang X, Wasti S, Lu S, ... Ozcan S (2023) *Materials Today* <https://doi.org/10.1016/j.mattod.2023.04.010>
44. Feng X, Wang X, Zhang C, Dang C, Chen Y, Qi H (2021) *Carbon* 183:187–195. <https://doi.org/10.1016/j.carbon.2021.07.022>
45. Perumal KS, Boopathi R, Selvarajan L, Venkataraman K (2023) The effects of zircon particles on the mechanical and morphological properties of glass fibre reinforced epoxy composite. *Mater Today Commun* 37:107067. <https://doi.org/10.1016/j.mtcomm.2023.107067>

**Publisher's Note** Springer Nature remains neutral with regard to jurisdictional claims in published maps and institutional affiliations.

Springer Nature or its licensor (e.g. a society or other partner) holds exclusive rights to this article under a publishing agreement with the author(s) or other rightsholder(s); author self-archiving of the accepted manuscript version of this article is solely governed by the terms of such publishing agreement and applicable law.